Phytomedicine 110 (2023) 154637

Contents lists available at ScienceDirect

Phytomedicine

journal homepage: www.elsevier.com/locate/phymed

Original Article

Novel chemical-structure TPOR agonist, TMEA, promotes megakaryocytes differentiation and thrombopoiesis *via* mTOR and ERK signalings

Xueqin Jiang [c,1], Yueshan Sun [d,1], Shuo Yang [a,1], Yuesong Wu [a], Long Wang [a], Wenjun Zou [e], Nan Jiang [a], Jianping Chen [f], Yunwei Han [g], Chunlan Huang [g], Anguo Wu [a,*], Chunxiang Zhang [a,*], Jianming Wu [a,b,*]

[a] *Key Laboratory of Medical Electrophysiology of Ministry of Education of China, Medical Key Laboratory for Drug Discovery and Druggability Evaluation of Sichuan Province, School of Pharmacy, Southwest Medical University, Luzhou, Sichuan 646000, China*
[b] *School of Basic Medical Sciences, Southwest Medical University, Luzhou, China*
[c] *State Key Laboratory of Biotherapy and Cancer Center, West China Medical School, Sichuan University, Chengdu, Sichuan 610041, China*
[d] *The Third People's Hospital of Chengdu, Chengdu, Sichuan 610031, China*
[e] *School of Pharmacy, Chengdu University of Traditional Chinese Medicine, Chengdu, Sichuan 611137, China*
[f] *School of Chinese Medicine, The University of Hong Kong, Hong Kong, China*
[g] *The Affiliated Hospital of Southwest Medical University, Luzhou, Sichuan 646000, China*

ARTICLE INFO

Keywords:
Megakaryocytes differentiation
Machine learning
Thrombocytopoiesis
3,4,3′-tri-o-methylellagic acid
Sanguisorba officinalis
Thrombopoietin receptor

ABSTRACT

Background: Non-peptide thrombopoietin receptor (TPOR) agonists are promising therapies for the mitigation and treatment of thrombocytopenia. However, only few agents are available as safe and effective for stimulating platelet production for thrombocytopenic patients in the clinic.
Purpose: This study aimed to develop a novel small molecule TPOR agonist and investigate its underlying regulation of function in megakaryocytes (MKs) differentiation and thrombopoiesis.
Methods: A potential active compound that promotes MKs differentiation and thrombopoiesis was obtained by machine learning (ML). Meanwhile, the effect was verified in zebrafish model, HEL and Meg-01 cells. Next, the key regulatory target was identified by Drug Affinity Responsive Target Stabilization Assay (DARTS), Cellular Thermal Shift Assay (CETSA), and molecular simulation experiments. After that, RNA-sequencing (RNA-seq) was used to further confirm the associated pathways and evaluate the gene expression induced during MK differentiation. In vivo, irradiation (IR) mice, C57BL/6N-TPOR^{em1cyagen} (*Tpor*$^{-/-}$) mice were constructed by CRISPR/Cas9 technology to examine the therapeutic effect of TMEA on thrombocytopenia.
Results: A natural chemical-structure small molecule TMEA was predicted to be a potential active compound based on ML. Obvious phenotypes of MKs differentiation were observed by TMEA induction in zebrafish model and TMEA could increase co-expression of CD41/CD42b, DNA content, and promote polyploidization and maturation of MKs in HEL and Meg-01 cells. Mechanically, TMEA could bind with TPOR protein and further regulate the PI3K/AKT/mTOR/P70S6K and MEK/ERK signal pathways. *In vivo*, TMEA evidently promoted platelet regeneration in mice with radiation-induced thrombocytopenia but had no effect on *Tpor*$^{-/-}$ and C57BL/6 (WT) mice.
Conclusion: TMEA could serve as a novel TPOR agonist to promote MKs differentiation and thrombopoiesis *via* mTOR and ERK signaling and could potentially be created as a promising new drug to treat thrombocytopenia.

Abbreviations: AI, Artificial intelligence; CETSA, Cellular Thermal Shift Assay; DARTS, Drug Affinity Responsive Target Stabilization Assay; DAPI, 4′, 6-diamidino-2-phenylindole dihydrochloride; MKs, Megakaryocytes; ML, Machine learning; MD, Molecular dynamics; MM/GBSA, Molecular mechanics/Generalized born surface are; PBS, Phosphate buffered saline; PDB, Protein Database Bank; qRT-PCR, Quantitative reverse transcription-polymerase chain reaction; RMSD, Root-mean-square deviation; TPO, Thrombopoietin; TPOR, Non-peptide thrombopoietin receptor; TMEA, 3,4,3′-Tri-O-methylellagic acid; SD, Standard deviation; VMD, Visual Molecular Dynamicsa.

* Correspondence authors at: Department of Pharmacology, School of Pharmacy, Southwest Medical University, Luzhou, Sichuan 646000, China.
E-mail addresses: wag1114@foxmail.com (A. Wu), zhangchx999@163.com (C. Zhang), jianmingwu@swmu.edu.cn (J. Wu).
[1] These authors contributed equally to this work.

https://doi.org/10.1016/j.phymed.2022.154637
Received 22 September 2022; Received in revised form 12 December 2022; Accepted 28 December 2022
Available online 28 December 2022
0944-7113/© 2022 Elsevier GmbH. All rights reserved.

Introduction

Thrombocytopenia, as a longstanding clinical dilemma, is the primary cause of bleeding (Aster et al., 2009; Xu et al., 2020). Thrombocytopenia has been implicated in diverse physiological and pathophysiological processes, including various inflammations and innate immune responses, especially for the risk of excess bleeding (Khan et al., 2020; Nicolai et al., 2019). Despite the fact that platelet transfusion is a powerful approach for severe thrombocytopenia, but it may cause severe hematogenous infections and immune reactions (Desborough et al., 2016; Levy et al., 2018). Hematopoietic stem cells undergo a series of developmental steps that result in the release of platelets from mature MKs. These processes include the proliferation of megakaryocyte progenitor cells, their differentiation, and their maturity into functional platelets (Bianchi et al., 2016). In order to treat clinical thrombocytopenia, increasing platelet production has been proved to be a successful method. Recently, a new therapy is mainly focused on increasing circulation of thrombopoietin (TPO) levels or stimulating TPOR, thereby increasing platelet production (Bussel et al., 2019; Li and Zheng, 2014). The activity of a TPOR agonist is similar to that of endogenous TPO, which can boost platelet counts and minimize the requirement for platelet transfusion (Chou and Mulloy, 2011; Ghanima et al., 2019; Ikeda and Miyakawa, 2009; Michel M, 2020). Therefore, TPOR agonists have been developed as promising therapies for relieving and treating thrombocytopenia.

Since the purification of TPO in 1994, TPOR agonists had undergone 2 generations of development and renewal as the peptide and non-peptide forms (Nakamura et al., 2006; Stasi et al., 2010). Although the first generation TPOR agonists, such as rhTPO and PEG-rHuMGDF, could elevate platelets, the potential immunogenicity of the patients hindered their widespread clinical application (Kuter, 2007; Kuter and Begley, 2002). To overcome this deficiency, the second generation of agents were developed, mainly including peptide and non-peptide mimetics (Stasi et al., 2010). Unfortunately, the peptide mimetics must be administered intravenously or subcutaneously and displayed potential risk of side effects, which limited their therapeutic effect and clinical application (Frederickson S, 2006). Furthermore, new oral non-peptides of TPO mimetics are currently clinically available for the treatment of thrombocytopenia (Koehrer et al., 2010). Recent data showed that 5 TPOR agonists have been approved for clinical treatment of thrombocytopenia worldwide, including 3 non-peptides of TPOR agonists (avatrombopag, lusutrombopag, and eltrombopag) and 2 peptides of TPOR agonists (romiplostim and rhTPO) (Ikeda and Miyakawa, 2009; Xie et al., 2018a). Consideration of only few drugs are available for stimulating platelet production with manageable adverse reactions in clinic, there is still an urgent need to discover and develop novel small molecule TPOR agonists for alleviating thrombocytopenia with less or no significant side effects.

Functional evidence has demonstrated that TPOR could be activated by binding its ligand TPO, followed by the activation of its downstream signaling pathways, including STAT3/5, AKT, and ERK signaling pathways (Chou and Mulloy, 2011; de Sauvage et al., 1994). Indeed, PI3K/AKT and MEK/ERK signaling pathways have been confirmed for their role in direct or indirect involvement in MKs proliferation, differentiation, maturation and platelet production (Chen et al., 2020). The activation of P70S6K by mTOR regulates the cell growth, which is vital for ribosome biogenesis and translational processes (Guglielmelli et al., 2011). Specially, the fate of hematopoiesis and MKs differentiation is largely orchestrated by a variety of transcription factors, such as *NF-E2, FLl-1*, and *GATA-1* (Elagib et al., 2003; Songdej and Rao, 2017). Nevertheless, the aforementioned networks regulated MKs differentiation and platelet formation have not been systematically investigated. Therefore, there is a compelling demand to further study the molecular mechanisms of TPOR agonists in the treatment of thrombopoiesis.

Traditional Chinese herbal medicine was considered a gold mine for the development of new treatments for various diseases, due to its miraculous effects (Yao et al., 2019). Presently, the clinical treatment with traditional Chinese medicine holds great potentials, especially complex diseases such as the treatment of hematological diseases. However, because of the diversity of the compositions in traditional Chinese medicine, making it difficult to explore which component plays a significant role. Faced with the low success rate of traditional screening technologies and the increasing R&D costs, recently, new drug screening technologies are imminent and more efficient and accurate platforms have emerged as the times require. With the improvement of computing power and the availability of big data, artificial intelligence (AI) technology, especially machine learning and deep learning, is one of the popular application directions in virtual drug screening (Prihoda et al., 2021). As a high-performance AI technology, machine learning with low cost in a short time could conceivably help to discover latent targets, confirm hits, and identify the effect of drugs (Elbadawi et al., 2020).

Here, we developed new robust and reliable models for screening compounds, with confirmed efficacy on promoting MKs differentiation and platelet production, and identified the TPOR as a novel and direct target for TMEA. TMEA, an ellagic acid, is isolated from the roots of traditional Chinese herb (*Sanguisorba Officinalis* L.) with hemostatic effects. *Sanguisorba Officinalis* L. has been widely used in clinic to treat various blood disorders in clinic, including hematemesis, epistaxis, hemorrhage, and hemorrhoids with bleeding, etc (Li et al., 2020; Su et al., 2019). We previously found that *Sanguisorba officinalis* L. had a definite curative effect on leukopenia, and significantly elevated the levels of platelets and red blood cells (Zhu et al., 2020). Further study demonstrated that the saponins extracted from *Sanguisorba officinalis* L. promoted the proliferation of bone marrow cells and enhanced platelets in mice (Chen et al., 2017). Moreover, we found that 2 ellagic acids isolated from the roots of *Sanguisorba officinalis* L. could promote proliferation of hematopoietic progenitor cells and MKs differentiation (Yan and Guo, 2004). Although the hematopoietic effect of ellagic acid is emerging, the underlying effect on promoting platelet production and especial mechanisms in the regulation of MKs differentiation and thrombopoiesis is still unknown.

By identification the activity *in vitro* and zebrafish model, we demonstrated that TMEA could promote platelet production. Mechanically, TMEA obviously promoted MKs polyploidization and maturation *via* targeting TPOR, thereby regulating the PI3K/AKT/mTOR/P70S6K and MEK/ERK signaling pathways. Furthermore, *in vivo* studies demonstrated TMEA evidently facilitated platelet recovery in mice with thrombocytopenia but had no effect on C57BL/6N-TPOR^{em1cyagen} (*Tpor*$^{-/-}$) and C57BL/6 (WT) mice. Our findings revealed that TMEA as a novel chemical-structure TPOR agonist promotes megakaryopoiesis and thrombopoiesis, which may provide new insights into the treatment of thrombocytopenia.

Materials and methods

Construction of ML-based drug screening models

The model structure diagram is presented in Fig. 1A. Firstly, we collected 41 small molecule compounds with MKs differentiation-promoting activity and 695 inactive small molecule compounds. Then 2 active and 10 inactive small molecule compounds were randomly selected from the compound library as test sets, and the remaining 724 small molecule compounds were used as training sets. Next, molecular descriptors were calculated using RDKit (http://www.rdkit.org). With RDKit calculations, we got 200 molecular descriptors for each compound. Molecular descriptors contain a variety of molecular properties, such as quantum electrodynamics (qed), molecular weight (MolWt), RingCount, LabuteASA, and BertzCT, among others. The Synthetic Minority Oversampling Technique (SMOTE) is used to balance the positive and negative of the samples. The active compound changed from 41 to 665, the inactive compound from 695 to 685, and the ratio of active to

inactive compound from 1:16.95 to 1:1.03. The molecular descriptors are then sorted using the Gini index, which is done by scoring each molecular descriptor using a random forest in RStudio, sorting the molecular descriptors of the 724 small molecule compounds in the training set from highest to lowest based on the size of the descriptor scores. Taking the molecular descriptor scores in the top 50%, 60%, 70%, 80%, 90%, and 100% of the total score, and generated 6 datasets. Finally, these 6 datasets were entered into the support vector machine model, and the optimal dataset was selected to train the support vector machine model and validate and predict the activity of the compound.

The prediction three-dimensional (3D) structure of TPOR and assessment

In brief, the amino acid sequence of TPOR was obtained from UniProt database and then used Iterative Threading Assembly Refinement (I-TASSER) server to obtain 3D structure prediction (Singh et al., 2016).

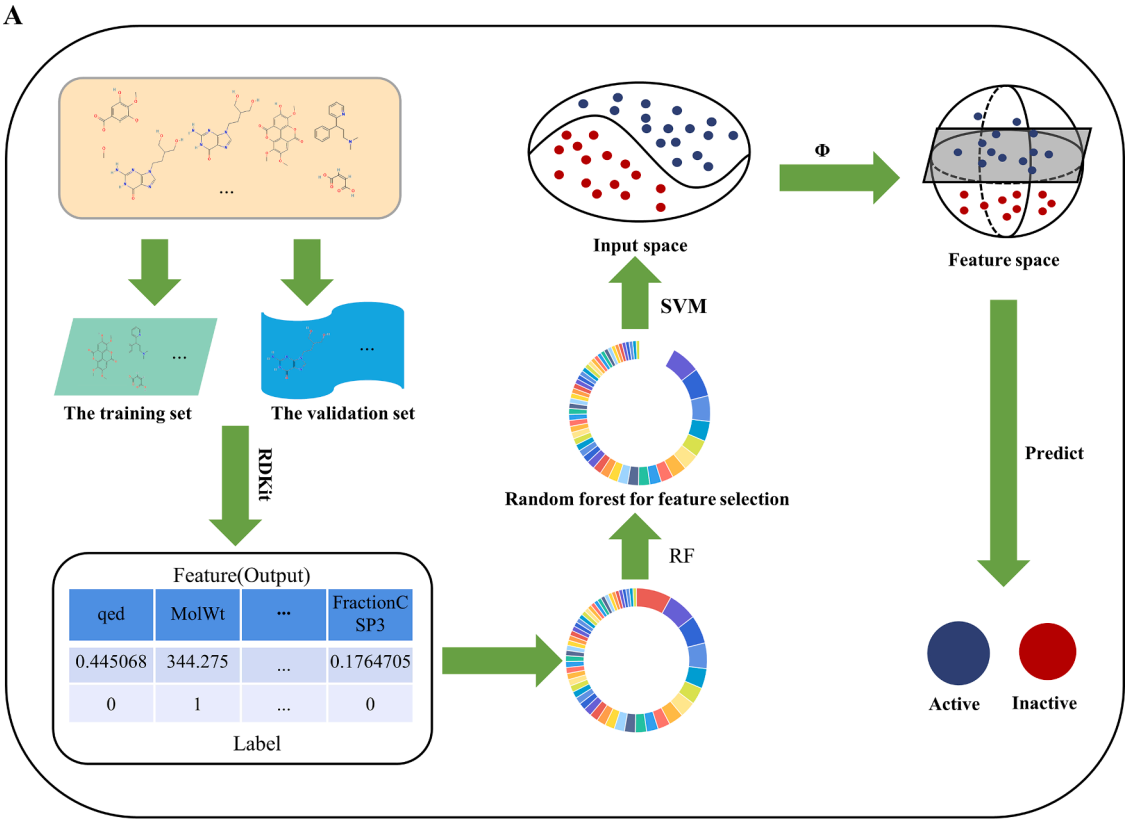

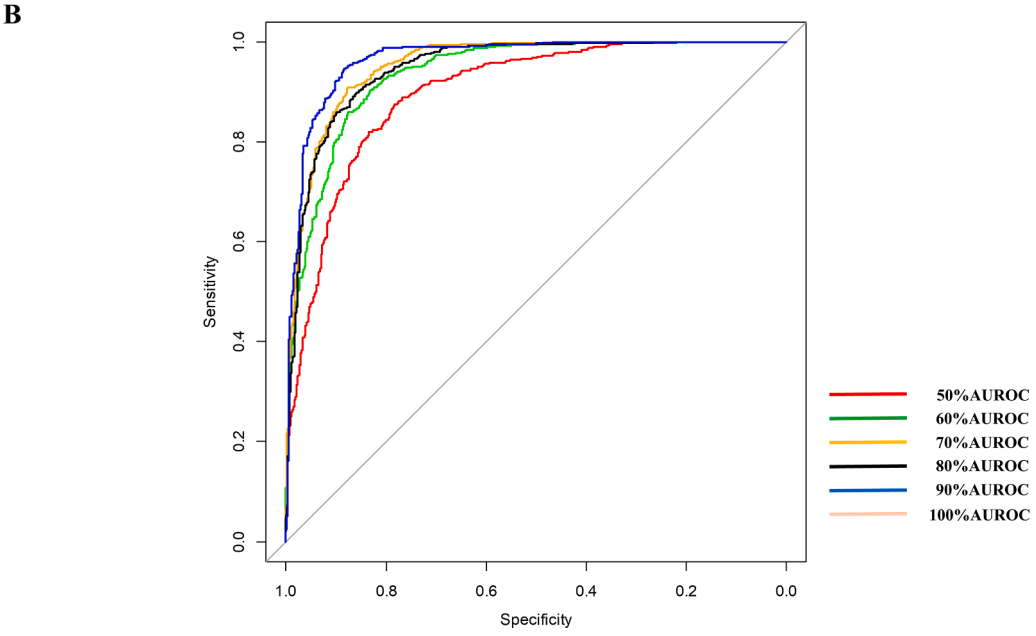

Fig. 1. Model construction of drug discovery and the authentication of active natural compounds. (A) Virtual Filter Flowchart. (B) ROC curves for different percentages of scores.

Next, the 3D conformation with the smallest absolute value of C-core was chosen for its protein sequence with good confidence level. Then, 3D structure was further assessed by SWISS-MODEL working space in automatic modeling pattern (http://swissmodel.expasy.org/workspace/). Predicted 3D structure was saved as PDB format. The structure of TMEA was downloaded from the RCSB protein data bank (Institute for Quantitative Biomedicine at Rutgers, Piscataway, NJ, USA). Subsequently, the optimized structure of TPOR obtained was added hydrogen atoms, adding charge and minimizing energy, and the binding modes and scores between TMEA and TPOR protein were evaluated using AutoDock 4.0 software. The structures were visualized by applying PyMol (Delano Scientific LLC, South San Francisco, CA)

DARTS

After culturation, Meg-01 cells were collected and split on ice with RIPA lysis buffer for 15 min. Centrifuge at 12,000 rpm for 15 min to obtain supernatant, and the protein concentration was tested using Bradford reagent and diluted to 5 mg/ml, then treated with TMEA or DMSO for 1 h at room temperature. Following this, pronase was appended various dilutions (1:600, 1:1200 and 1:1800) and incubation for 10 min at 40 ℃. Then, put 5 × loading buffer into sample and boil at 95 ℃ for 10 min. The sample proteins were analyzed by Western blotting.

CETSA

For CETSA experiments, Meg-01 cells were lysed by the above method. Then, the cell lysates were separated into two groups, one group was cultured with the DMSO as the control group and the other group was cultured with TMEA for 1 h as the TMEA-treated group (at 25 ℃). Then, the lysates of both groups were divided into equal portions, and then heated at successively higher temperatures (37-72 ℃) for 4 min. After boiling for 10 min, Western blot assays were taken to analyze the abundance levels of TPOR protein.

Zebrafish

TG (itga2b: EGFP) (also referred to as CD41: GFP) (Svoboda et al., 2014) zebrafish was selected in this experiment. Zebrafish were housed at 28.5 ℃ and kept on a 14 h light/10 h dark cycle at zebrafish core facilities of Southwest Medical University. Zebrafish mating, grading and rearing according to IACUC guidelines (Chiang et al., 2021; Grabher et al., 2011).

Study of thrombocytes in TG (itga2b: EGFP) transgenic zebrafish

After 3 days post fertilization (dpf) was suppressed by 0.05 μM Phenylthiourea (PTU), Tg (itga2b: EGFP) were placed under a confocal laser scanning microscope (TCS SP8; Leica, Wetzlar, Germany) to screen the positive zebrafish embryos with normal development and green fluorescence of platelets in blood circulation. The screened embryos were placed in a 6-well culture plate containing various drug concentrations or blank control (80 embryos in 8 ml of solution per well) group. After covering the fresh-keeping film, ventilated the hole on the fresh-keeping film, cultured in an incubation room (27–29 ℃). To keep the embryos healthy, the state was observed every day and pick out the dead embryo in time. After 5 dpf, the Tg (itga2b: EGFP) zebrafish were fixed at 4 ℃ overnight with 4% paraformaldehyde and CD41: GFP^{+} cells were examined by TCS SP8.

Observation of cells morphology

The morphology of HEL and Meg-01 cells was observed on days 8 and 12, and three randomly visual fields of each well were captured under a Nikon microscope (Nikon Corporation, Tokyo, Japan). Meanwhile, cells were respectively harvested and resuspended in phosphate buffered saline (PBS) and swelled with 0.075 M KCl solution, then fixation was performed with fixed solution (methanol: glacial acetic acid = 3:1). Cell suspension was placed dropwise on slides and stained with fresh Giemsa solution for 8 min. After that, the multinucleated MKs were captured by microscope.

Phalloidin staining

After 8 and 12 days of intervention, HEL and Meg-01 cells were harvested and fixed with 4% paraformaldehyde and dehydrated by precooled acetone (−20 ℃) for 15 min. Afterwards, the cells were colored with rhodamine-phalloidin (100 nM) for 1 h and restrained with 4′, 6-diamidino-2-phenylindole dihydrochloride (DAPI) for 5 min. Finally, the anti-fluorescence quencher was adopted to mount and visualize using fluorescence microscope (Leica Microsystems GmbH, Germany). Excitation was performed with 560 nm laser for phalloidin and DAPI at 405 nm.

Analysis of differentiation and DNA content

To determine the differentiation potency of TMEA, HEL and Meg-01 cells were collected on day 12 and stained with megakaryocytic markers FITC-anti-CD41 and PE-anti-CD42b (eBioscience, San Diego, USA) for 25 min at 4 ℃ according to the manufacturer's note, then unpacked by BD FACSVerse™ flow cytometer (BD Biosciences, San Jose, CA, USA). For DNA content determination, the cells were fixed with 70% ethanol precooled at 4 ℃ for at least 2 h, then incubated with 100 μl RNase at 37 ℃ for 30 min, followed by addition of 400 μl propidium iodide at 4 ℃ for 30 min in the dark, and then immediately collected for flow cytometry. Data were analyzed by FlowJo 7.6 software (FlowJo LLC., Ashland, OR, USA). Additionally, cells were separated and fixed with paraformaldehyde, stained with DAPI, and cell cycle and DNA content were evaluated by Acapella high content imaging and analysis software (Perkin Elmer, Woodbridge, ON, Canada).

Immunofluorescence staining

To investigate the nuclear translocation of transcription factors affecting MKs differentiation, cells were processed for immunofluorescence staining. The cells were attached to coverslips after experimental treatment for 12 days in total, which were fixed with 10% paraformaldehyde for 20 min, washed twice with PBS, and then permeabilized with 0.2% Triton X-100 for 10 min, and closed with 5% BSA for 60 min. The coverslips were followed by incubating with primary GATA-1/NF-E2/β1-tubulin antibody (1:200) overnight at 4 ℃ and stained with FITC-conjugated goat anti-Rabbit IgG secondary antibody and then added secondary FITC labeled goat anti-rabbit antibodies (1:200; Zhongshan Golden Bridge Biotechnology, Beijing, China) for 60 min, and counterstained with DAPI for 5 min. The slides were washed and analyzed under a fluorescence microscope with fluorescence detection excitation wavelengths (λ ex) were performed as follows: λ ex = 470 nm for FITC and λ ex = 405 nm for DAPI, respectively.

Transmission electron microscope

After TMEA (10 μM) treatment for 14 days, Meg-01 cells were collected and performed in 0.5% glutaraldehyde, and then fixed with 3% glutaraldehyde fixative. Ultrathin sections (50 nm) were observed and imaged under a JEM-1400PLUS transmission electron microscope (JEOL Ltd., Tokyo, Japan).

Quantitative reverse transcription-polymerase chain reaction (qRT-PCR)

Gene expression analysis was detected by qRT-PCR. First, we collected TMEA-intervened cells, extracted total RNA using TRIzol

reagent (Invitrogen, CA, USA) and used reverse transcription kits (Invitrogen, CA, USA) according to the manufacturer's directions, 1 μg of RNA was reverse transcribed into cDNA. Primers were designed by Primer Library and Primer-Blast. The primers were designed by Primer bank and Primer-Blast. Subsequently, qRT-PCR amplification was performed using SYBR® Green Master Mix (TIANGEN Biotechnology, Beijing, China), and each sample was performed with three replicates. The religious expression levels of target genes were determined by normalizing the response threshold cycle (C_T) values of targeted genes to the housekeeping gene glyceraldehyde 3-phosphate dehydrogenase (GAPDH). The primer sequences are shown in Supplementary Table 2.

RNA-sequencing

HEL cells were incubated with TMEA (10 μM) for 4 days, approximately 5×10^6 cells were collected and dissolved in 1 ml TRIzol reagent and quickly freezing in liquid nitrogen. Sample integrity assessment (Agilent, Walterbronn, Germany), library preparation and RNA-sequencing were performed on Illumina Hiseq 2500 platform (Illumina, San Diego, CA, USA) to be sequenced on the Novogene Bioinformatics Institute (Novogene Biotech Co., Ltd., Beijing, China) to generate 150 bp paired-end (PE150) reads. Use the free online platform (https://magic.novogene.com) to carry out analysis of the data.

Western blotting analysis

Western blotting analysis as described previously (Teng et al., 2020). Briefly, HEL cells were harvested on days 4, 8 and 12 after treatment with TMEA, and washed with PBS and then subjected to lysis for 15 min on ice with RIPA lysis buffer (Cell Signaling Technology, Beverly, MA, USA) which contained a mixture of protease inhibitor cocktail without EDTA (TargetMol, Shanghai, China). The supernatants were gathered after being centrifuged at 12,000 rpm for 10 min at 4 ℃, and protein concentrations were measured using the Quick Start™ Bradford 1× Dye Reagent (Bio-Rad, Hercules, CA, USA). Meanwhile, the supernatants were then mixed with 5× loading buffer then heated at 95 ℃ for 10 min. Subsequently, the samples were briefly loaded on SDS-PAGE gels and then transferred onto PVDF membranes (Pall Life Sciences, Massachusetts, US). After that, they were closed with 5% skim milk powder in PBST for 1 h and incubated with primary antibodies (1:1000) overnight at 4 ℃, then with appropriate secondary antibodies. The intensity of protein bands was observed using UltraSignal™ ECL Western blotting detection reagents (4A Biotech Co., Ltd, Beijing, China) and quantified by ImageJ software (National Institutes of Health, Bethesda, MD, USA). In addition, the proportion of gray value of the target protein band over that of β-actin was indicated as the relative expression level of target protein.

Animal experiments

Kunming mice, aged 6–8 weeks, were used in the animal experiment and purchased from Dashuo Company (Dasuo Biological Technology Co., LTD, Chengdu, Sichuan, China), C57BL/6N-TPOR^{em1cyagen} (TPOR$^{-/-}$) mice and C57BL/6 (WT) mice were bought from Cyagen Biosciences Company (Cyagen Biosciences Inc., Guangzhou, Guangdong, China). Kunming mice were treated with 4 Gy total body irradiation (IR) by a medical linear accelerator (Precise accelerator, Elekta, Sweden), and were selected randomly into six groups: normal mice treated with saline, IR mice treated with saline, TPO (3000 U/kg), and TMEA (2.5, 5, 10 mg/kg), respectively. The *Tpor*$^{-/-}$ and WT mice were separated into three groups: saline, TPO (3000 U/kg), and TMEA (10 mg/kg). The committee for the use of animal care at Southwest Medical University, Luzhou, China, approved the experimental methods for all animal care in this experiment (No. 20170306).

Platelet counts and organ value analysis in mice

The mice were injected intraperitoneally for 14 days. Blood was obtained from the orbital venous plexus on the specified days, and platelets were analyzed by a multi-parameter automatic hematology analyzer (Sysmex XT-2000iV, Kobe, Japan). After recovery to normal platelets level, mice were killed by cervical dislocation and vital organs were carefully extracted and weighed.

Statistical analysis

Statistics were performed using GraphPad Prism software version 8.0 (San Diego, CA, USA). One-way and Two-way analysis of variance (ANOVA) were performed to examine statistical differences. At minimum three individual experiments were taken in this subject, and the outcomes were presented as mean ± standard deviation (SD). Data with statistical meaningfulness was set at $p < 0.05$.

Results

Drug screening model construction based on support vector machine and virtual screening of active natural chemicals

In this study, SVM was employed to build drug screening models (Fig. 1A). For the SVM model, the prediction score for each molecule is between 0 and 1, and the model decision is made with the threshold 0.5. The molecule showing a score above the 0.5 threshold was identified as an active compound. After obtaining 6 datasets (Fig. 1B), the 6 datasets were entered into the SVM model, and the optimal model was selected for the next experiment. First evaluating the predictive performance of these training sets, we found that the dataset with a score of 90% gave the model the best predictive performance, and when the support vector machine's $C = 10$ and $\gamma = 5.6$, its area under the curve (AUC) value reached 0.967. To further validate the performance of the model, a test set containing 2 active compounds and 10 inactive compounds was fed into the model. The results showed that the prediction accuracy of the model is 100%. Finally, the model was used to predict the activity of 1968 compounds in the Discovery Probe FDA-approved Drug Library, with 87 compounds having biological activity that promoted MK differentiation or platelet production. Among them, the predicted score of TMEA was 0.549847, which was active.

The identification of TMEA

Sanguisorba officinalis L. was used to separate and extract TMEA according to previous studies (Bai et al., 2019; Yan and Guo, 2004). The data were shown by UHPLC-QTOF-MS/MS and NMR chromatograms in Supplementary Fig. 1, which was consistent with those of the previous reports of TMEA. Through further separation, purification and identification, the structure of TMEA is 3,3 ', 4 '-O-trimethylellagic acid and the molecular formula is $C_{17}H_{12}O_8$. Meanwhile, the purity of TMEA was determined to be above 98.35% based on a peak area normalization method detected by LC analysis.

TMEA directly targets TPOR

To investigate whether TMEA interacts specially with the TPOR to promote MKs differentiation, we explored molecular docking analysis. The results showed that TMEA directly interacted with TPOR through four hydrogen bonds with good docking score (Fig. 2A), suggesting that TMEA may interact directly with TPOR. Then, DARTS assay was employed to verify the potential protein target in thrombopoiesis. We observed that a concentration-dependent increase in the stability of TPOR against pronase after treatment with TMEA but not DMSO (Fig. 2B-C). To obtain further evidence for the targeting of TMEA to TPOR, the CETSA experiment was performed. As seen in Fig. 2D, the

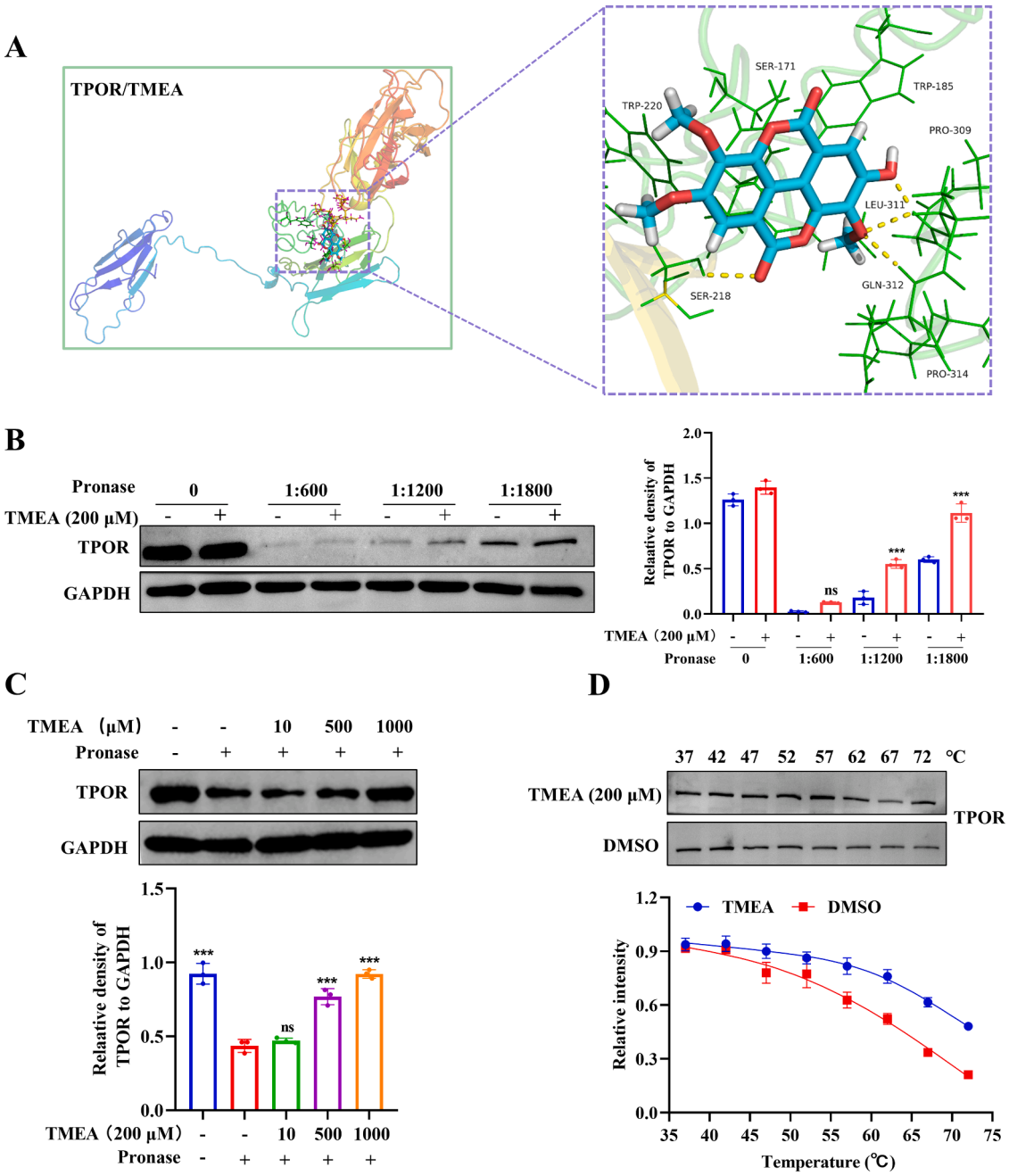

Fig. 2. TMEA directly targets TPOR. (A) Conformation of the TPOR protein bound to TMEA in a three-dimensional structural diagram determined by molecular docking analysis. (B-C) The DARTS analysis for target verification. In Meg-01 cells lysates, several dilutions (1:600, 1:1200 or 1:1800) in protease 50 μg/ml stock solution were added into the control and TMEA (200 μM) intervention groups at 40 ℃ for 10 min. TMEA treatment led to an enhanced stability of TPOR protein (B). After treating both groups with protease (1:1000) for 10 min, the DARTS results showed that the stability of TPOR became more stable with increasing doses of TMEA (C). (D) CETSA analysis of TPOR degradation damage by different temperatures. $n = 3$, mean ± SD. Statistical contrasts were subjected to one-way ANOVA with Turkey's multiple-comparisons test. ***$p < 0.001$ vs. the indicated group.

addition of TMEA to heat-denatured Meg-01 cells lysates led to the stabilization of TPOR at various temperatures. Collectively, these information taken together showed that TMEA is specifically targeting TPOR.

TMEA promotes MKs differentiation

Compared with cell and mouse models, zebrafish exhibited high throughput, drug delivery, biology and target, and has become the used widely and core technologies for drug candidate discovery. We discovered that TG (itga2b: EGFP) placed in various concentrations of TMEA medicines dramatically increased the number of GFP^+ cells at 5 dpf, which represent HSPCs and platelets (Fig. 3A), indicating that TMEA grows HSPCs and thrombocytes in zebrafish embryos. To evaluate the effect of TMEA on MKs differentiation, the cytotoxicity of TMEA was initially evaluated in HEL and Meg-01 cells by LDH assay. As shown in supplementary Fig. 2A, TMEA up to 20 μM exhibited only minimal cytotoxicity against the cells at days 4, 8, and 12. Therefore, we selected 10 and 20 μM of TMEA for the subsequent *in vitro* study (Byrne et al., 2020). Additionally, the cells started to proliferate on day 4 and TMEA inhibited the growth of HEL and Meg-01 cells (Supplementary Fig. 2B). TMEA (10 and 20 μM) and PKC412 (150 nM, a known megakaryocytic

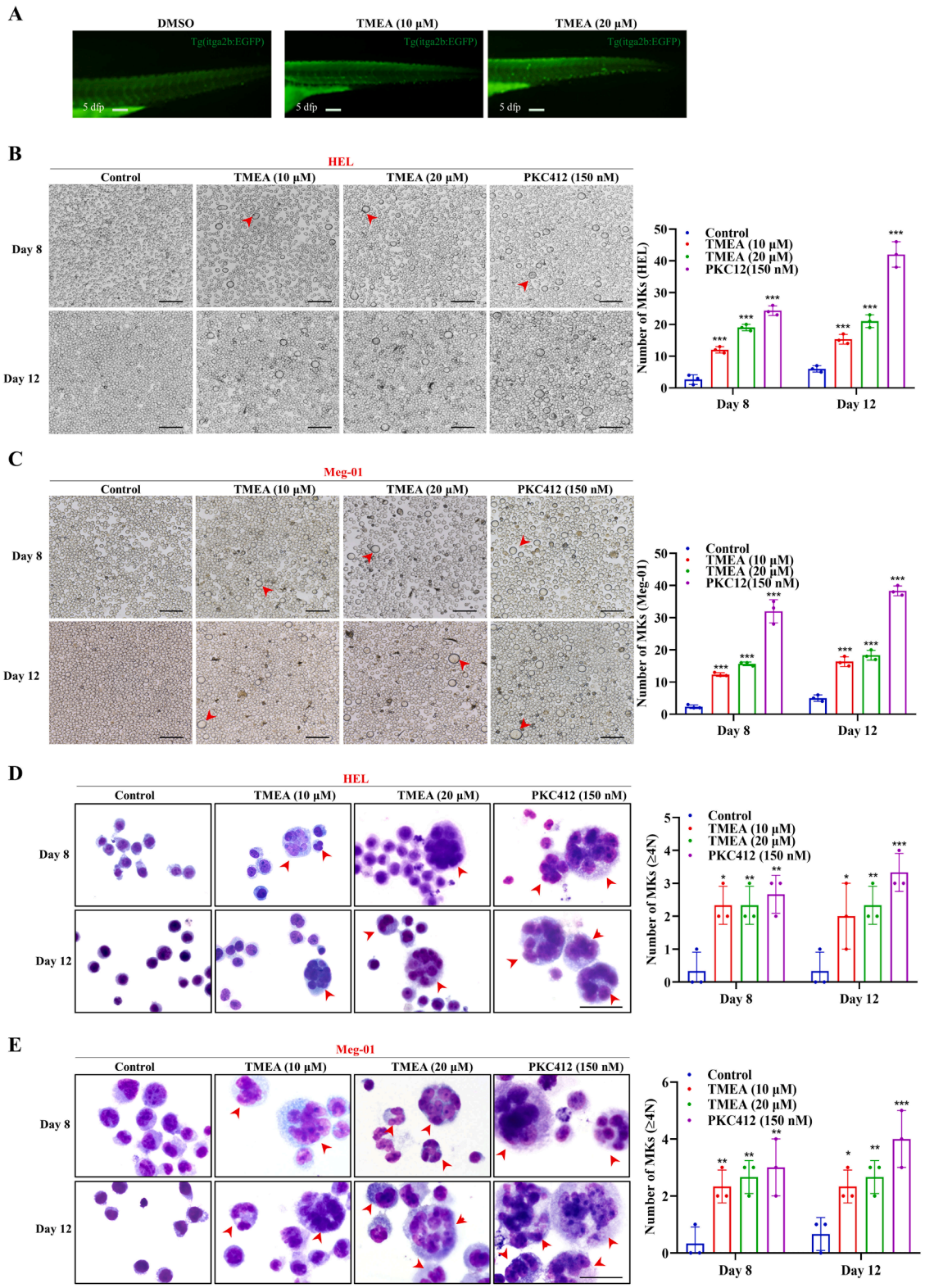

Fig. 3. TMEA induces dramatic morphological changes and differentiation. (A) TMEA was shown to increase the number of platelets and HSPCs in the developing zebrafish embryo. CD41: GFP^{+} cells in 5 dpf zebrafish embryos were placed in drug concentration groups or blank control. (B-C) The effects of TMEA and PKC412 on cells size and morphological variations. The cells were randomly examined at visual fields of each well under a Nikon microscope. Magnification: 200×, scale bar: 100 μm. The red arrows indicate large multinucleated cells. The percentage of polyploid MKs were shown in Bar graphs. vs. the control. (D-E) The images of MKs stained by Giemsa staining under a light microscope. Magnification: 400×, Scale bar: 100 μm. The thick red arrows indicate large-sized MKs with polyploid nuclei. $n = 3$, mean ± SD. Statistical comparisons were detected by Two-way ANOVA with the Tukey's multiple comparisons test, $^{*}p < 0.05$, $^{**}p < 0.01$, $^{***}p < 0.001$ vs. the control.

differentiation inducer as positive control (Huang et al., 2009,) significantly increased the number of large-sized MKs on days 8 and 12 (Fig. 2B-C), but only few cells with size increases were observed under a microscope on day 4 in previous exploration. Furthermore, the nuclear-to-cytoplasm ratio, large-sized cells, and deeply-stained multilobulated nuclei were obviously increased by Giemsa staining (Fig. 2D-E). The data suggest that TMEA could promote MKs differentiation.

TMEA induces MKs-typical differentiation and polyploidization

CD41 and CD42b are specific surface antigens of MKs, and DNA ploidy is an indispensable indicator for MKs maturation. Therefore, we further determined the action of TMEA on the co-expression of CD41/CD42b and DNA content compared to that of PKC412 in HEL and Meg-01 cells on day 12 by flow cytometry. TMEA and PKC412 obviously increased the percentage of $CD41^{+}CD42b^{+}$cells (Fig. 4A), and the population of $\geq$ 4 N DNA content (Fig. 4B). Similarly, TMEA markedly increased the fraction of polyploid cells and decreased the proportion of depolyploidized cells in HEL and Meg-01 cells by high-content imaging analysis (Fig. 4C-D).

The process of MKs maturation was accompanied by polyploidization of the nucleus and release of cytoplasm-specific particles (Kosoff et al., 2015). To evaluate the effect of TMEA-induced polyploidization, the actin cytoskeleton was visualized by phalloidin staining. Multinucleated actin ring formation was clearly observed following TMEA and PKC412 treatment in HEL and Meg-01 cells on day 8 (Fig. 5A), and polylobulated nuclei cells with dilated cytoplasm were more prominent on day 12 (Fig. 5B). The data indicate that TMEA could promote polyploidization and maturation of MKs.

TMEA induces the mRNA expression and nuclear translocation of NF-E2 and GATA-1

Transcription factors including *NF-E2, FLl-1, RUNX1* and *GATA-1* play a pivotal role in mediating the specification, differentiation of MKs and platelet production (Maroni, 2019; Szalai et al., 2006). Therefore, we investigated the mRNA expressions of *NF-E2, FLl-1, RUNX1* and *GATA-1* and nuclear translocations of *NE-E2* and *GATA-1* in HEL and Meg-01 cells. The results showed TMEA (10 μM) significantly up-regulated the mRNA expressions of *NF-E2, FLl-1, RUNX1* and *GATA-1* (Fig. 5C-D). Moreover, TMEA (10 and 20 μM) and PKC412 (150 nM) induced significant accumulation of *NF-E2* and *GATA-1* in the nuclei with bright fluorescence, which was stronger than that in the cytoplasm (Fig. 5E-F). The data suggest that TMEA could promote the mRNA expression and nuclear translocation of the related transcription factors to induce MKs maturation and platelet production.

TMEA regulates the mTOR and ERK pathways

To study the molecular mechanism by that TMEA promotes MKs differentiation, the mRNA expressions were analyzed by RNA-sequencing technology. The levels of gene expression were distinguishable between TMEA and the control (Fig. 6A). A total of 4595 mRNAs were aberrantly expressed including 2415 up-regulated and 2180 down-regulated after TMEA treatment (Fig. 6B), which were significantly enriched in biological processes (BPs), cellular components (CCs), and molecular functions (MFs) (Fig. 6D). In addition, MKs-associated signaling pathways (JAK-STAT, PI3K-AKT-mTOR, and MAPK) were obviously enriched by KEGG analysis (Fig. 6C). Taken together, these data indicate that TMEA has the potential for the regulation of MKs-affiliated proteins. Next, we investigated the effect of TMEA on signaling pathways involved with MKs differentiation. We found that TMEA significantly increased the phosphorylation of PI3K, AKT, mTOR, P70S6K, MEK and ERK in HEL cells on days 8 and 12 (Fig. 6E), implying that TMEA activates the PI3K/AKT/mTOR/P70S6K and MEK/ERK signaling pathways. Furthermore, pretreatment with LY294002 (a PI3K inhibitor) for 6 h, then TMEA-induced for 6 days in the presence of LY294002, significantly restrained the expression of PI3K, AKT, mTOR, and P70S6K in HEL cells (Fig. 6F). Similarly, U0126 (an ERK1/2 inhibitor) also blocked the effects of TMEA on the expressions of ERK and NF-E2 proteins (Fig. 6G). Then, Molecular docking was performed to prove whether TMEA binds to MKs-associated proteins such as PI3K, AKT, mTOR, MEK, and ERK or not. The hydrogen bonds between TMEA and MKs-associated proteins could be clearly observed with high docking combination scores (Supplementary Fig. 3A and Table 3). The binding free energy (ΔGbind) $<$ -20 kcal/mol and corresponding energy components were depicted in Supplementary Table 4. Furthermore, the root-mean-square deviation (RMSD) of TMEA fluctuated near 0.5 Å, and the proteins and complexes kept stable (Supplementary Fig. 3B). The root-mean-square fluctuation (RMSF) of these proteins was low (Supplementary Fig. 3C), and the visual molecular dynamic trajectories were displayed in Supplementary material (Videos 1–6). The data indicate that TMEA could regulate MKs-associated proteins. These information are identical with the data of KEGG analysis and proved that TMEA could activate the mTOR and ERK signaling pathways.

TMEA facilitates the formation of proplatelet and platelet

It is known that activation of TPOR triggers the expression of transcription factors that take part in the megakaryocytic pathways, thereby promoting platelet production (Szalai et al., 2006). In the present study, TMEA obviously up-regulated the phosphorylation levels of STAT3, STAT5, GATA-1 and NF-E2 (Fig. 7A). Rac/Cdc42 is crucial for platelet production, particularly for the regulation of microtubule dynamics (Pleines et al., 2013). TMEA significantly increased the levels of phosphorylated Rac/Cdc42, TPOR, and β1-tubulin in HEL cells (Fig. 7B-C). Furthermore, the cytoplasm of protruded filaments, nuclear fluorescence and MKs polyploid were significantly increased in HEL and Meg-01 cells by the imaging of β1-tubulin-labeled platelet as green color (Fig. 7D), indicating the typical features of proplatelet formation (Patel-Hett et al., 2008; Thon and Italiano, 2012). Moreover, TMEA induced the typical morphological changes of platelet including membrane architecture and numerous granules (Fig. 7E). These results suggest that TMEA might facilitate the development of MKs into proplatelets and platelets.

TMEA accelerates platelet recovery in IR mice in vivo

Platelets are derived from specialized precursor cells, MKs, which reside in bone marrow (Sim et al., 2016). Therefore, we tested the influence of TMEA on promoting platelet production in mice with severe thrombocytopenia brought on by 4 Gy IR (Fig. 8A). TMEA and TPO were efficacious in promoting platelet production and resumption in IR mice (Fig. 8C). In addition, a progressive recovery of white blood cells was also found in IR mice administrated with TMEA (5 and 10 mg/kg) (Supplementary Fig. 4B). However, no significant difference was found in red blood cell counts (Supplementary Fig. 4C). Additionally, the body weights of mice were relatively constant during 14 days administration of TMEA or TPO (Fig. 6D). Interestingly, the ratio of liver to body weight (liver index) was higher after TPO or TMEA administration than that of saline injection (control) in IR mice (Supplementary Fig. 4A, 2D), suggesting that TMEA and TPO may have protective effects on the liver following IR-induced injury (Kim and Jung, 2017). Furthermore, we found that TMEA markedly elevated the expression of TPOR protein (Supplementary Fig. 4 G). The data indicate that TMEA could promote platelet production and recovery as well as protect against liver damage in IR mice.

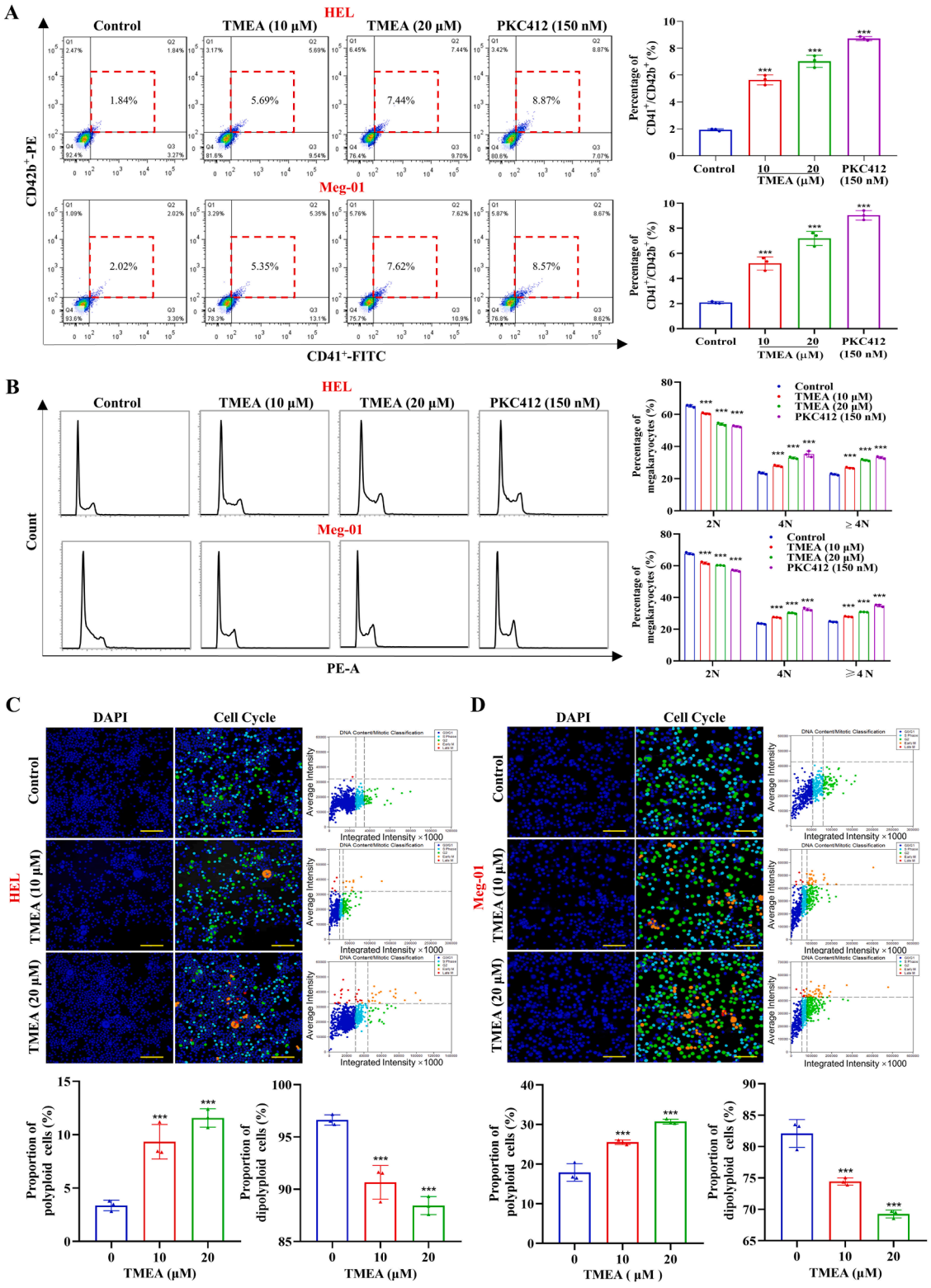

Fig. 4. TMEA differentially induces MKs-typical differentiation. The percentage of $CD41^{+}CD42b^{+}$ complexes surface expression on MKs (A) and DNA content (B). The cells were treated with TMEA (10 and 20 μM) or PKC412 (150 nM) for 12 days and analyzed by flow cytometry; The ploidy distribution (left) shows the number of cells in each ploidy level and the representative DNA histogram (right) indicates the percentage of polyploid cells. DAPI staining, cycle distribution and polyploid cells could be visualized in HEL (C) and Meg-01 (D) cells, and histogram represents the proportion of dipolyploid and polyploid cells in every group. $n = 3$, mean ± SD. Statistics were determined by one-way ANOVA with Dunnett's and two-way ANOVA with Tukey's multiple comparisons test, $^{***}p < 0.001$ vs. the control.

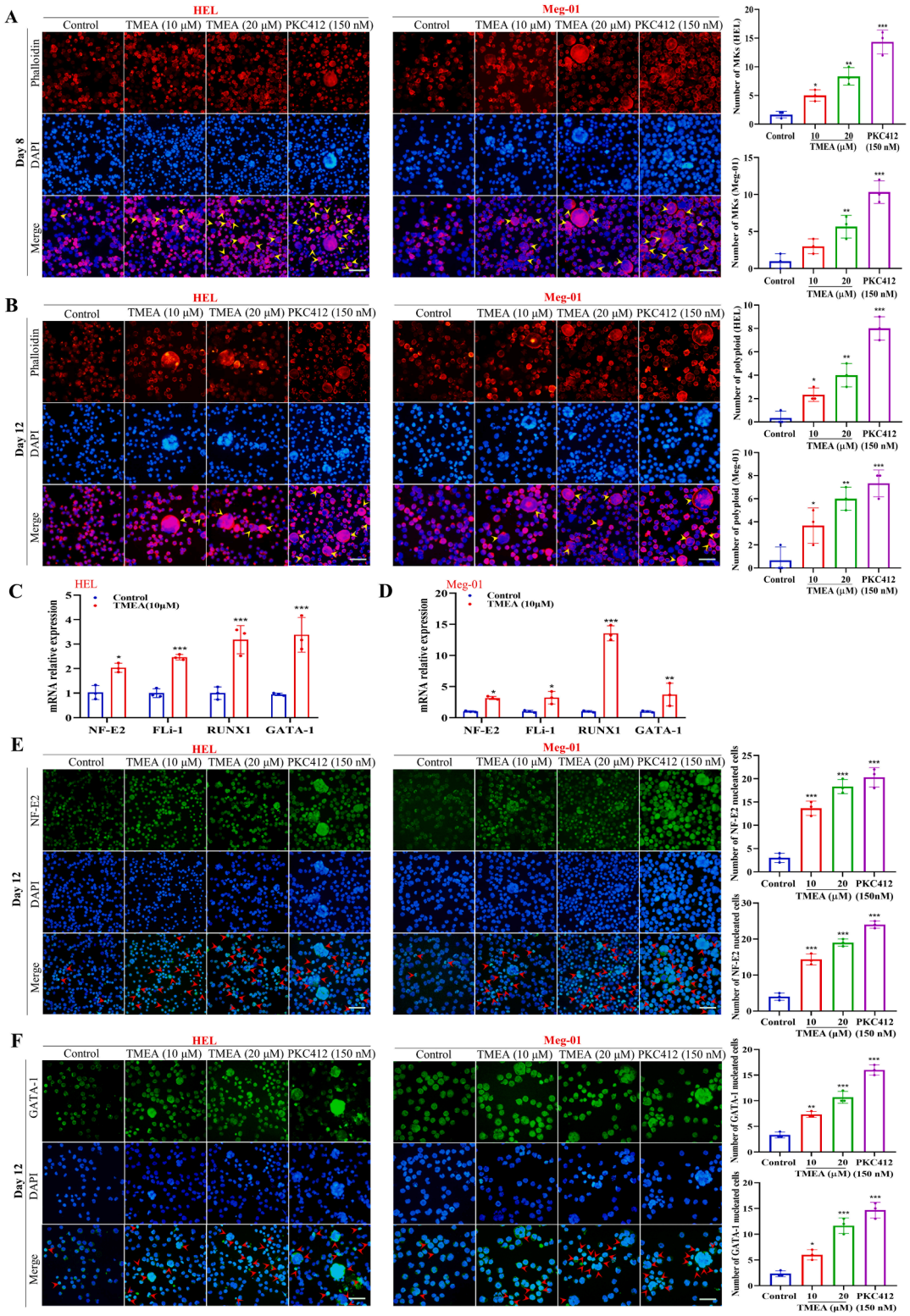

Fig. 5. TMEA facilitates polyploidization and induces the nuclear translocation of *NF-E2* and *GATA-1*. Phalloidin-labeled cytospin in HEL and Meg-01 cells on days 8 (A) and 12 (B) under a fluorescence Microscope (excitation wavelength: 560 nm for Phalloidin, 405 nm for DAPI). Magnification: 400×, Scale bar: 50 μm. Yellow arrows indicate representative actin polymerization and polyploidization of MKs. The ratio of mRNA levels of *NF-E2, FLI-1, RUNX1* and *GATA-1* relative to *GAPDH* after HEL (C) and Meg-01 (D) cells were treated with TMEA for 4 days. GAPDH was employed as a loading comparison. (E-F) Representative immunofluorescence image (left) and biochemical quantification (right) of the nuclear translocation of *NF-E2* and *GATA-1* in HEL and Meg-01 cells upon treatment with TMEA for 12 days. The red arrows indicate the nuclear translocation of the transcription factor (excitation wavelength: 470 nm for FITC and 405 nm for DAPI, Magnification: 400×, Scale bar: 50 μm). The volume of transcription factors *NF-E2* and *GATA-1* entering the nuclei of HEL and Meg-01 cells is shown in the right-hand bar graph, respectively. $n = 3$, mean ± SD. Statistics were determined by one-way ANOVA with Dunnett's and two-way ANOVA with Tukey's multiple comparisons test, $^{*}p < 0.05$, $^{**}p < 0.01$, and $^{***}p < 0.001$ vs. the control.

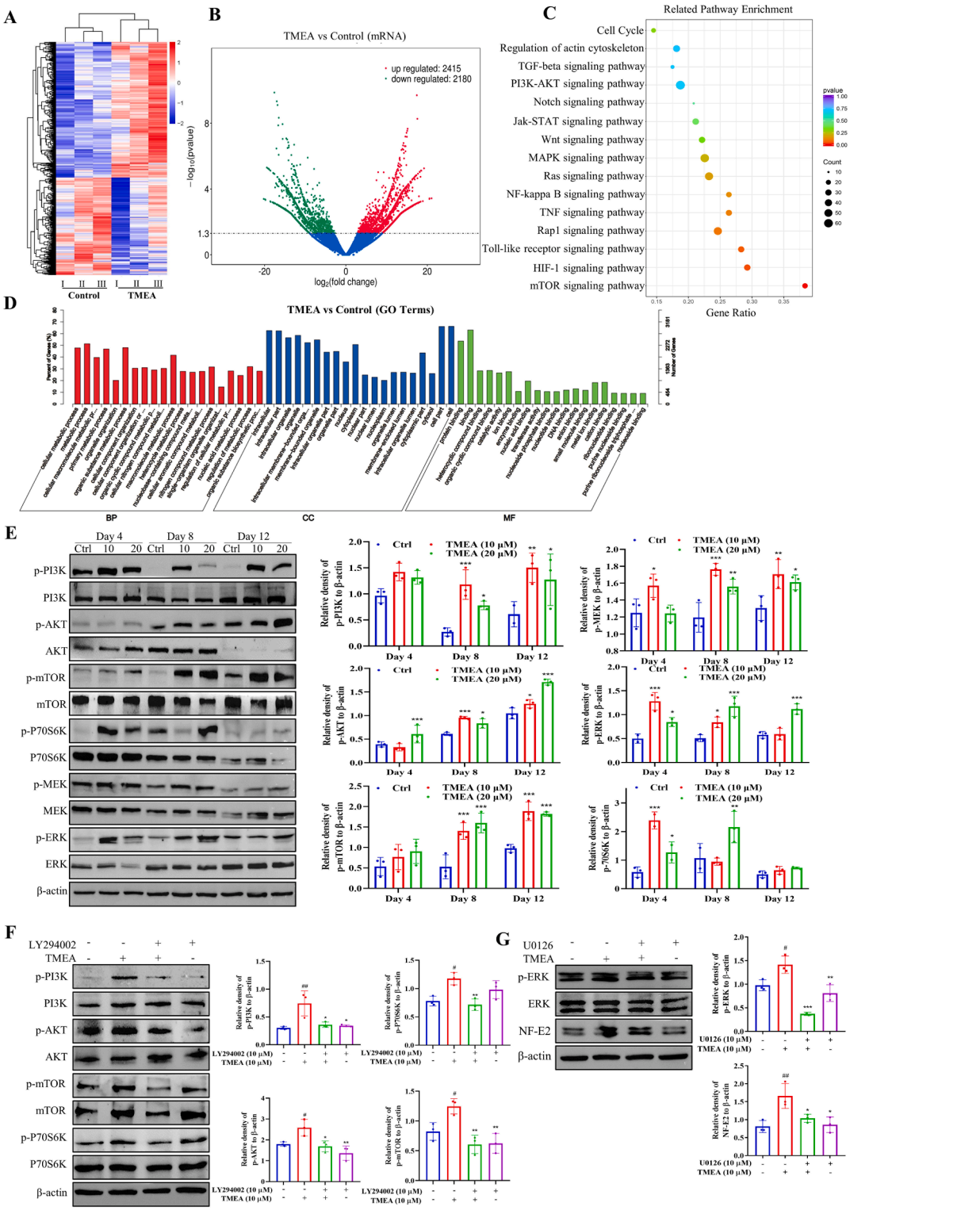

Fig. 6. TMEA promotes MKs differentiation *via* regulating mTOR and ERK signaling pathways in HEL cells. (A) Differential mRNAs expression by Heatmap. (B) Differential mRNAs expression by Volcano plot. (C) The up-regulated mRNAs associated with MKs differentiation-related pathways by KEGG analysis. (D) The differential mRNAs were considerably concentrated in biological processes (BP), cellular components (CC), and molecular function (MF) from GO results. (E) Representative immunoblot images and biochemical quantification of MKs-affiliated pathway proteins (mTOR and ERK pathways) after treatment with TMEA (10 and 20 μM) in HEL cells for 4, 8 and 12 days. $n = 3$, mean ± SD; $^{*}p < 0.05$, $^{**}p < 0.01$, and $^{***}p < 0.001$ vs. the control. (F-G) HEL cells were pretreated with LY294002 (10 μM) or U0126 (10 μM) for 6 h followed by TMEA-induced (10 μM) in the presence or absence of inhibitor for 6 days, and the levels of associated proteins were detected by Western blotting. (F) The expressions of p-PI3K, PI3K, p-AKT, AKT, p-mTOR, mTOR, p-P70S6K, P70S6K, and β-actin after treatment with TMEA ± LY294002. (G) The expressions of p-ERK, ERK, NF-E2 and β-actin after treatment with TMEA and/or U0126. $n = 3$, mean ± SD; $^{\#}p < 0.05$, $^{\#\#\#}p < 0.001$, vs. the control; $^{*}p < 0.05$, $^{**}p < 0.01$, and $^{***}p < 0.001$ vs. TMEA alone. $n = 3$, mean ± SD. Statistical comparisons were performed using ANOVA test.

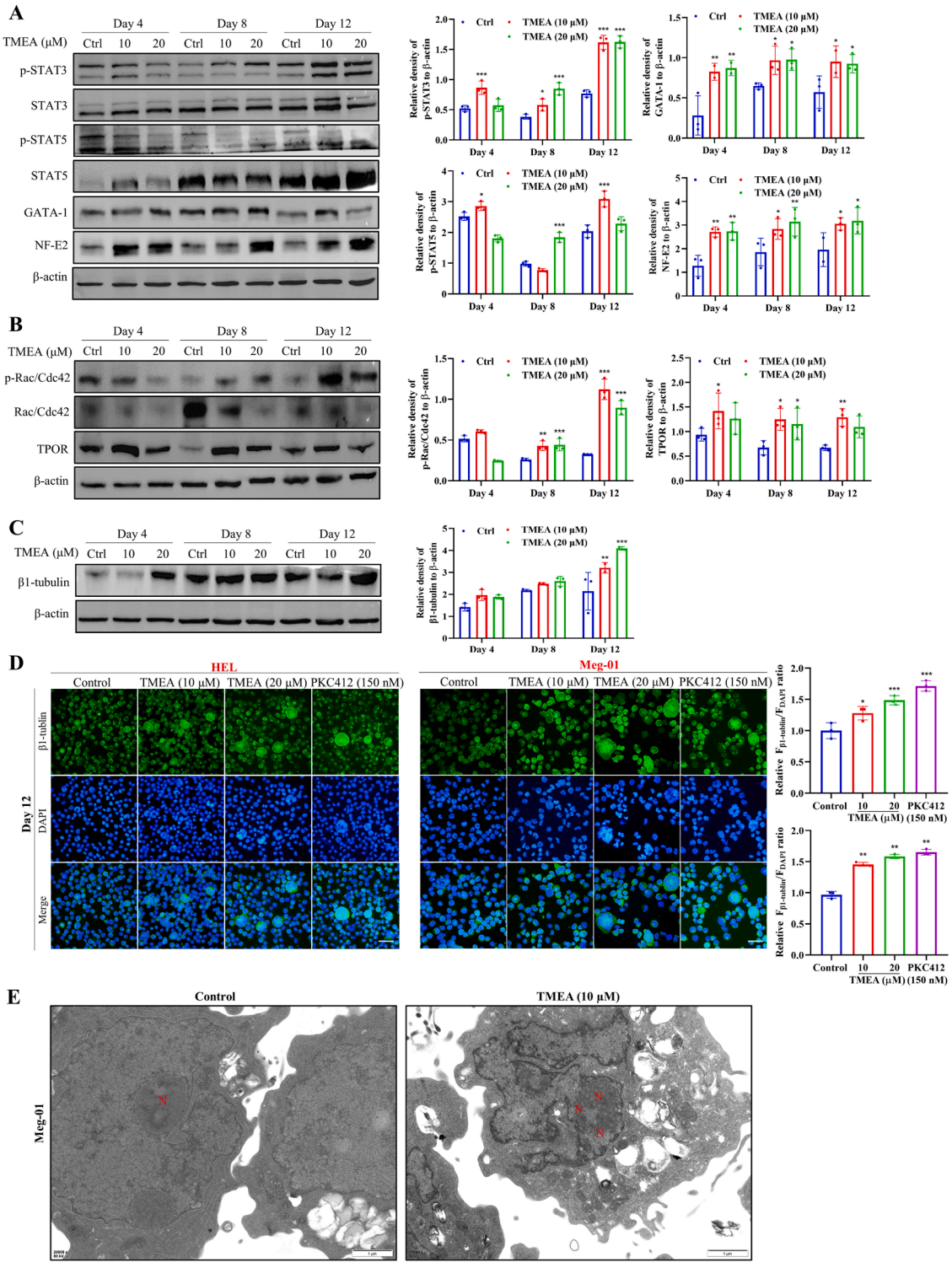

Fig. 7. TMEA up-regulates the expressions of transcription factors and promotes proplatelet and platelet formation. (A) The protein levels of transcription factors p-STAT3, STAT3, p-STAT5, STAT5, GATA-1, and NF-E2. (B) The expressions of proplatelet-related proteins p-Rac/Cdc42, Rac/Cdc42 and TPOR in HEL cells following treatment with TMEA (10 and 20 μM) for 4, 8 and 12 days. (C-D) Representative immunoblot and immunofluorescence images of proplatelet production-related proteins (β1-tublin). Excitation wavelength: 470 nm for FITC and 405 nm for DAPI, Magnification: 400×, Scale bar: 50 μm. (E) Images of Meg-01 cells treated with TMEA (10 μM) on day 14 under a transmission electron microscopy; Magnification: 20,000×, Scale bar: 1 μm, N: nucleus. $n = 3$, mean ± SD. Statistics were determined by one-way ANOVA with Dunnett's and two-way ANOVA with Tukey's multiple comparisons test, $^{*}p < 0.05$, $^{**}p < 0.01$, and $^{***}p < 0.001$ vs. the control.

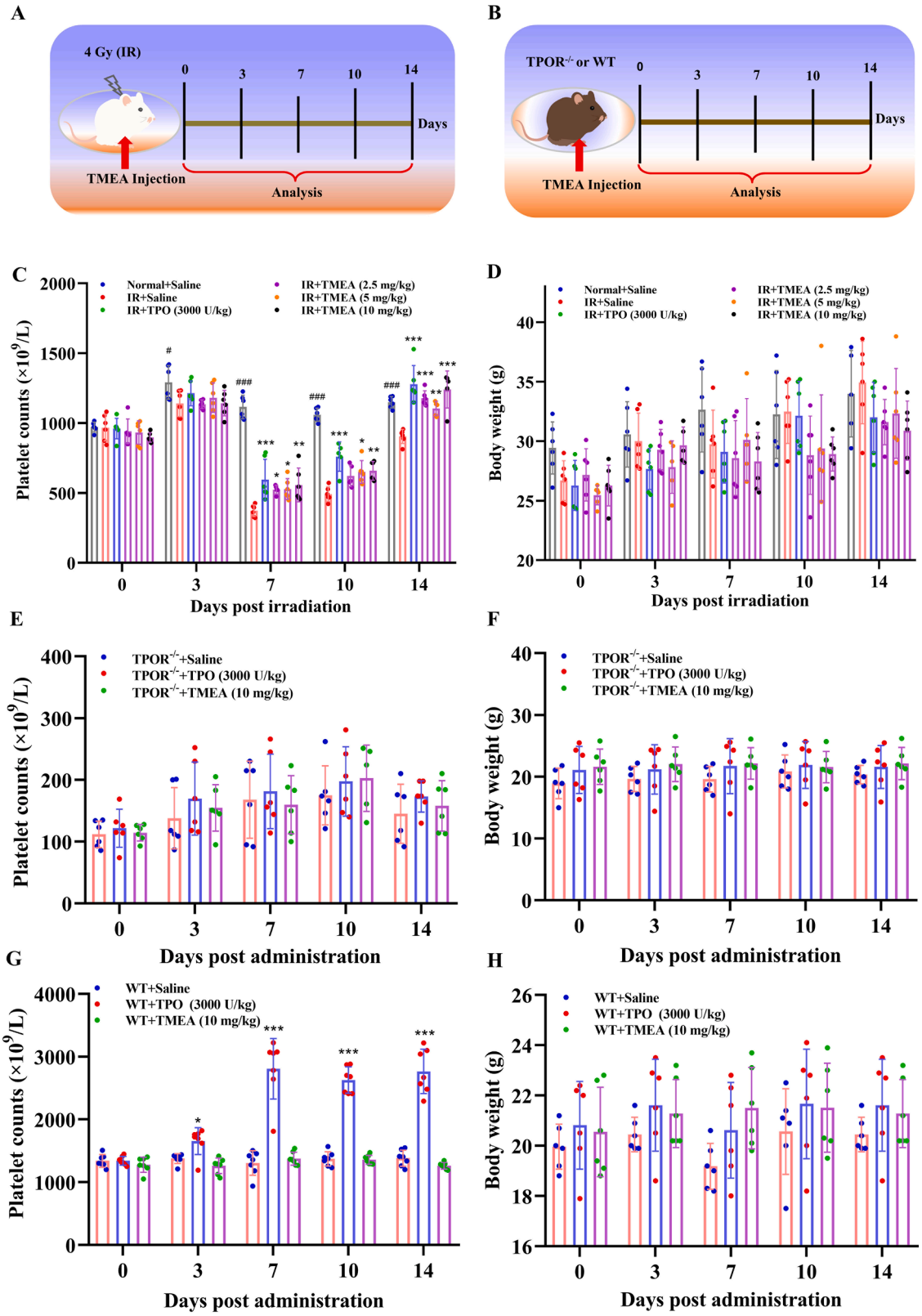

Fig. 8. TMEA promotes platelet recovery in IR mice. Mice ($n = 8$) were exposed on day 0, followed by intraperitoneal injection of saline, thrombopoietin (TPO, 3000 U/kg), or TMEA (2.5, 5, and 10 mg/kg). Peripheral blood and body weight were measured on days 0, 3, 7, 10, and 14. (A) Experimental schematic of TMEA administration in Kunming mice subjected to 4 Gy IR. (B) Experimental schematic of TMEA administration in C57BL/6N-TPOR^{em1cyagen} (*Tpor*$^{-/-}$) and C57BL/6 (WT) mice. (C) Altered peripheral platelet counts in IR mice undergoing TMEA delivery. (D) The body weight of IR mice that received TMEA injection. (E) Variations in peripheral platelet counts in *Tpor*$^{-/-}$ mice after TMEA and TPO stimulation. (F) The body weight of *Tpor*$^{-/-}$ mice that received TMEA and TPO injection. (G) Changes in the peripheral platelet counts in WT mice receiving TMEA and TPO stimulation. (H) The body weight of WT mice receiving TMEA and TPO injection. $n = 6$, Data are expressed as mean ± SD. Two-way ANOVA with Tukey's multiple comparisons test was used unless otherwise specified, $^{*}p < 0.05$, $^{**}p < 0.01$, and $^{***}p < 0.001$, vs. IR (saline); $^{\#}p < 0.05$, and $^{\#\#\#}p < 0.001$, normal (saline) vs. IR (saline).

TMEA make no difference on platelet generation in TPOR$^{-/-}$ and WT mice

To study whether TMEA-induced MKs differentiation and platelet formation are associated with the TPO/TPOR signal or not, we evaluated the effect of TMEA on platelet production and compared to that of TPO in *Tpor*$^{-/-}$ and WT mice (Fig. 8B). TMEA did not change the level of platelets in *Tpor*$^{-/-}$ and WT mice (Fig. 8E-G). However, TPO increased platelet production for 2-fold in wild type mice, but had no effect on *Tpor*$^{-/-}$ mice. Moreover, the body weight and organ index were relatively constant without significant changes in all groups (Fig. 8F-H, and Supplementary Fig. 4E-F). The results indicated that TMEA facilitates platelet production *via* activating the TPO/TPOR signaling.

Discussion

Traditional therapy of thrombocytopenia was to reduce platelet destruction or transfusion of platelets (Portielje et al., 2001). Since platelet transfusion caused various adverse reactions, stimulating platelets formation is the potential strategy in clinic (Cantoni et al., 2015). The TPOR could mediate the signaling functions of TPO in regulating MKs differentiation and platelet production (Chou and Mulloy, 2011). Therefore, the research and development of targeted small-molecule TPOR agonists has been an alternative approach to treat thrombocytopenia. So far, only 3 oral nonpeptide TPOR agonists such as avatrombopag, lusutrombopag, and eltrombopag are considered as attractive drugs to treat thrombocytopenia (Bussel et al., 2014; Ghanima et al., 2019; Michel M, 2020). Compared with peptides, nonpeptide agonists of TPOR have better oral bioavailability and extremely low probability of inducing immune response (Jenkins et al., 2007; Nakamura, 2008; Nogami et al., 2008). Here, we find TMEA from *Sanguisorba Officinalis* L., as a novel chemical-structure TPOR agonist that promotes MKs differentiation and thrombopoiesis.

Firstly, we developed a more efficient and accurate SVM construct drug screening model, a supervised machine learning technique algorithm, to gain natural compounds with hematopoietic activity. Interestingly, we obtained a novel-structure compound, TMEA, has biological activity to promote MKs differentiation or thrombopoiesis from traditional Chinese medicine for the first time. Secondly, consideration that the function of TPOR agonists mimics the action of endogenous TPO, which can increase platelet production. We further examined whether TMEA served as a TPOR agonist to promote platelet production. According to our molecular docking analysis, we found that TMEA might have interaction with TPOR protein. DARTS is a marker free compound identification method based on the change of protein proteolytic susceptibility (Lomenick et al., 2009). CETSA is an unbiased cell-based method, which aims to the thermal stability of protein induced by compounds, as to verify the interaction between compounds and cell protein targets (Molina et al., 2013). TMEA markedly protected TPOR protein against degradation and increased the thermal stability that further verified the protein is the target of TMEA, as evidenced by a good molecular interaction network, indicating that TMEA could activate TPOR to regulate MKs differentiation.

Furthermore, compared with mouse models, the combined advantages of *in vivo* complexity and *in vitro* high-throughput screening convenience of zebrafish make it a prominent vertebrate model for research in various fields including developmental biology, toxicology and drug discovery. Previous study showed that they constructed TG (CD41: EGFP) zebrafish and explored the activation of lysophosphatidic acid receptor 3 to inhibit megakaryocyte production (Lin et al., 2018). Consistent with these reports, in this assay, by examining the CD41: GFP^{+} cells in zebrafish embryos, we observed as a candidate drug observing that TMEA expanded HSPCs and thrombocytes. Not only, *in vivo* experiment, we combined IR and *Tpor*$^{-/-}$ mice to jointly verify the efficacy of TMEA in promoting platelet formation.

Additionally, previous study has reported that the TPO activates TPOR to trigger intracellular signaling cascades including the STAT, AKT, and ERK pathways, thereby contributing to MKs differentiation and thrombocytopoiesis (Basson, 2012). Likewise, through RNA-sequencing analysis and further validation, we demonstrated that the potential effect of TMEA on the signaling pathways associated with differentiation, and displayed that TMEA can activate the JAK-STAT, PI3K-AKT-mTOR and MAPK signaling pathways, which has been shown to promote thrombopoiesis (Wang et al., 2022; Woods et al., 2019; Xie et al., 2018b). Notably, we found that TMEA increased the expression of TPOR, indicating that TMEA activated TPOR with similar kinetics to TPO. Most importantly, a profound inhibition of proteins was found in PI3K and ERK signaling pathways. Therefore, TMEA regulates MKs differentiation *via* the mTOR and ERK signaling pathways, as similar molecular mechanism (activating TPOR receptor), but structurally different to TPO. Interestingly, we also demonstrated that TMEA has a good binding affinity with above target proteins (PI3K, AKT, mTOR, MEK, ERK1/2) by molecular docking and dynamics simulation. However, we did not analyze the detailed interaction of TMEA with these proteins, and it needs to be further investigated.

We demonstrated that TMEA as a novel chemically structured small molecule TPOR agonist could activate TPOR signaling, further promoted MKs differentiation and platelet production through modulating mTOR and ERK signaling pathways (Fig. 9). However, TMEA did not trigger an unexpected severe excessive increase of platelet level in the normal body of mice. The arguments for this conclusion still worthy of consideration and further exploration. And the demonstration of *in vitro* mechanisms still requires extensive biological replication, such as direct Drug-target binding (such as SPR, surface plasmon resonance), as well as the development of other cellular models (such as human CD34 hematopoietic progenitor cells).

Conclusion

In conclusion, our study proves that *Sanguisorba Officinalis* L.-derived TMEA is a novel TPOR agonist that significantly promotes megakaryocytes differentiation *in vitro* without toxicity, facilitates the production of zebrafish GFP:CD41^{+} cells, and platelet recovery in radiation-injured mice, but not in TPOR$^{-/-}$ mice. Combined with our target validation experiments on the promotion of MKs differentiation by TMEA, we conclude that *Sanguisorba Officinalis* L.-derived TMEA, as a novel TPOR agonist, can activate the PI3K/Akt/mTOR and MEK/ERK signaling pathways to promote MKs differentiation and platelet production.

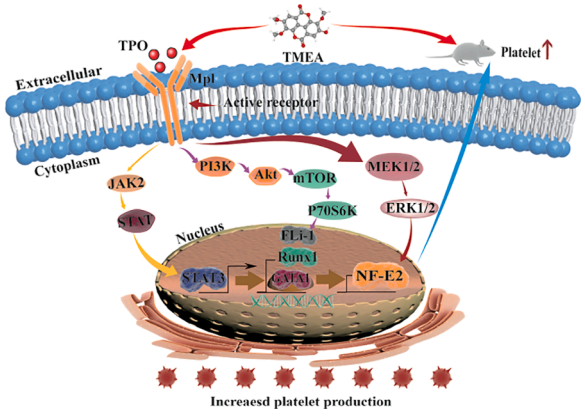

Fig. 9. Schematic illustration of the TMEA-induced signaling pathways in modulating megakaryocytes differentiation and platelets production *via* activating TPOR. TMEA could bind with TPOR protein and regulate the PI3K/AKT/mTOR/P70S6K and MEK/ERK signal pathways, further increasing the expression of transcription factors, thereby stimulating platelets production.

CRediT authorship contribution statement

Xueqin Jiang: Conceptualization, Data curation, Formal analysis, Writing – original draft, Writing – review & editing. **Yueshan Sun:** Data curation, Formal analysis, Writing – original draft, Writing – review & editing. **Shuo Yang:** Data curation, Formal analysis, Writing – original draft, Writing – review & editing. **Yuesong Wu:** Writing – review & editing, Formal analysis. **Long Wang:** Writing – review & editing, Formal analysis. **Wenjun Zou:** Conceptualization, Resources, Methodology. **Nan Jiang:** Writing – review & editing, Formal analysis. **Jianping Chen:** Conceptualization. **Yunwei Han:** Conceptualization. **Chunlan Huang:** Conceptualization. **Anguo Wu:** Conceptualization, Investigation, Writing – review & editing. **Chunxiang Zhang:** Conceptualization, Resources, Methodology. **Jianming Wu:** Conceptualization, Funding acquisition, Resources, Writing – review & editing.

Confilcts of interest

This manuscript has been reviewed and checked by all the authors. Meanwhile, all the authors agree to submit to *Phytomedicine*. We have read and understood *Phytomedicine*'s policies, and we believe that neither the manuscript nor the study violates any of these. There are no conflicts of interest to declare.

Acknowledgments and Funding

The authors thank Professor Can Tang for authenticating the dried roots of *Sanguisorba officinalis* L. used in this study. We also thank Yangshen He for the NMR analysis.

This work was supported by grants from National Natural Science Foundation of China (Grant Nos. 82074129 and 81804221); Science and Technology Planning Project of Sichuan Province, China (Grant Nos. 2022JDJQ0061 and 22ZYZYTS0191); joint project of Luzhou Municipal People's Government and Southwest Medical University, China (Grant Nos. 2020LZXNYDZ03 and 2020LZXNYDP01).

Supplementary materials

Supplementary material associated with this article can be found, in the online version, at doi:10.1016/j.phymed.2022.154637.

References

Aster, R.H., Curtis, B.R., McFarland, J.G., Bougie, D.W., 2009. Drug-induced immune thrombocytopenia: pathogenesis, diagnosis, and management. J. Thromb. Haemost. 7, 911–918.

Bai, C., Sun, Y., Pan, X., Yang, J., Li, X., Wu, A., Qin, D., Cao, S., Zou, W., Wu, J., 2019. Antitumor effects of trimethylellagic acid isolated from *Sanguisorba officinalis* L. on colorectal cancer via angiogenesis inhibition and apoptosis induction. Front. Pharmacol. 10, 1646.

Basson, M.A., 2012. Signaling in cell differentiation and morphogenesis. Cold Spring Harb. Perspect. Biol. 4, a008151.

Bianchi, E., Norfo, R., Pennucci, V., Zini, R., Manfredini, R., 2016. Genomic landscape of megakaryopoiesis and platelet function defects. Blood 127, 1249–1259.

Bussel, J., Kulasekararaj, A., Cooper, N., Verma, A., Steidl, U., Semple, J.W., Will, B., 2019. Mechanisms and therapeutic prospects of thrombopoietin receptor agonists. Semin. Hematol. 56, 262–278.

Bussel, J.B., Kuter, D.J., Aledort, L.M., Kessler, C.M., Cuker, A., Pendergrass, K.B., Tang, S., McIntosh, J., 2014. A randomized trial of avatrombopag, an investigational thrombopoietin-receptor agonist, in persistent and chronic immune thrombocytopenia. Blood 123, 3887–3894.

Byrne, A.J., Bright, S.A., McKeown, J.P., O'Brien, J.E., Twamley, B., Fayne, D., Williams, D.C., Meegan, M.J., 2020. Design, synthesis and biochemical evaluation of novel ethanoanthracenes and related compounds to target Burkitt's Lymphoma. Pharmaceuticals 13, 16.

Cantoni, S., Carpenedo, M., Mazzucconi, M.G., De Stefano, V., Ruggeri, M., Vianelli, N., Zaja, F., Barcellini, W., Nichelatti, M., Coccini, V., Baldacci, E., Rossi, E., Puglisi, S., Ciminello, A., Cairoli, R., 2015. Thrombopoietin Receptor Agonist (TPO-RA) switch in adult primary immune thrombocytopenia (ITP) patients: a retrospective collaborative survey from 8 Italian hematology centers. Blood 126.

Chen, S.L., Qi, Y., Wang, S., Xu, Y., Shen, M.Q., Hu, M.J., Du, C.H., Chen, F., Chen, M., Lu, Y.K., Zhang, Z.H., Quan, Y., Wang, C., Wang, F.C., Wang, J.P., 2020. Melatonin enhances thrombopoiesis through ERK1/2 and Akt activation orchestrated by dual adaptor for phosphotyrosine and 3-phosphoinositides. J. Pineal Res. 68, e12637.

Chen, X., Li, B., Gao, Y., Ji, J., Wu, Z., Chen, S., 2017. Saponins from *Sanguisorba officinalis* improve hematopoiesis by promoting survival through FAK and Erk1/2 activation and modulating cytokine production in bone marrow. Front. Pharmacol. 8, 130.

Chiang, J.C., Chen, W.M., Lin, K.H., Hsia, K., Ho, Y.H., Lin, Y.C., Shen, T.L., Lu, J.H., Chen, S.K., Yao, C.L., Chen, B.P.C., Lee, H.Y., 2021. Lysophosphatidic acid receptors 2 and 3 regulate erythropoiesis at different hematopoietic stages. BBA, 1866, 158818.

Chou, F.S., Mulloy, J.C., 2011. The thrombopoietin/MPL pathway in hematopoiesis and leukemogenesis. J. Cell. Biochem. 112, 1491–1498.

de Sauvage, F.J., Hass, P.E., Spencer, S.D., Malloy, B.E., Gurney, A.L., Spencer, S.A., Darbonne, W.C., Henzel, W.J., Wong, S.C., Kuang, W.J., et al., 1994. Stimulation of megakaryocytopoiesis and thrombopoiesis by the c-Mpl ligand. Nature 369, 533–538.

Desborough, M.J.R., Smethurst, P.A., Estcourt, L.J., Stanworth, S.J., 2016. Alternatives to allogeneic platelet transfusion. Br. J. Haematol. 175, 381–392.

Elagib, K.E., Racke, F.K., Mogass, M., Khetawat, R., Delehanty, L.L., Goldfarb, A.N., 2003. RUNX1 and GATA-1 coexpression and cooperation in megakaryocytic differentiation. Blood 101, 4333–4341.

Elbadawi, M., Gaisford, S., Basit, A.W., 2020. Advanced machine-learning techniques in drug discovery. Drug Discov. Today 26, 769–777.

Frederickson S, R.M., Lin, B., Smith, L.M., Calveley, P., Springhorn, J.P., Johnson, K., Wang, Y., Su, X., Shen, Y., Bowdish, K.S., 2006. A rationally designed agonist antibody fragment that functionally mimics thrombopoietin. Proc. Natl. Acad. Sci. U. S. A. 103, 5.

Ghanima, W., Cooper, N., Rodeghiero, F., Godeau, B., Bussel, J.B., 2019. Thrombopoietin receptor agonists: ten years later. Haematologica 104, 1112–1123.

Grabher, C., Payne, E.M., Johnston, A.B., Bolli, N., Lechman, E., Dick, J.E., Kanki, J.P., Look, A.T., 2011. Zebrafish microRNA-126 determines hematopoietic cell fate through c-Myb. Leukemia 25, 506–514.

Guglielmelli, P., Barosi, G., Rambaldi, A., Marchioli, R., Masciulli, A., Tozzi, L., Biamonte, F., Bartalucci, N., Gattoni, E., Lupo, M.L., Finazzi, G., Pancrazzi, A., Antonioli, E., Susini, M.C., Pieri, L., Malevolti, E., Usala, E., Occhini, U., Grossi, A., Caglio, S., Paratore, S., Bosi, A., Barbui, T., Vannucchi, A.M., Investigators, A., 2011. Safety and efficacy of everolimus, a mTOR inhibitor, as single agent in a phase 1/2 study in patients with myelofibrosis. Blood 118, 2069–2076.

Huang, Y.C., Chao, D.K., Clifford Chao, K.S., Chen, Y.J., 2009. Oral small-molecule tyrosine kinase inhibitor midostaurin (PKC412) inhibits growth and induces megakaryocytic differentiation in human leukemia cells. Toxicol. in Vitro 23, 979–985.

Ikeda, Y., Miyakawa, Y., 2009. Development of thrombopoietin receptor agonists for clinical use. J. Thromb. Haemost. 7 (Suppl 1), 239–244.

Jenkins, J.M., Williams, D., Deng, Y.L., Uhl, J., Kitchen, V., Collins, D., Erickson-Miller, C.L., 2007. Phase 1 clinical study of eltrombopag, an oral, nonpeptide thrombopoietin receptor agonist. Blood 109, 4739–4741.

Khan, R., Menard, M., Jen, C.C., Chen, X., Norris, P.A.A., Lazarus, A.H., 2020. Inhibition of platelet phagocytosis as an in vitro predictor for therapeutic potential of RBC antibodies in murine ITP. Blood 135, 2420–2424.

Kim, J., Jung, Y., 2017. Radiation-induced liver disease: current understanding and future perspectives. Exp. Mol. Med. 49, e359.

Koehrer, S., Keating, M.J., Wierda, W.G., 2010. Eltrombopag, a second-generation thrombopoietin receptor agonist, for chronic lymphocytic leukemia-associated ITP. Leukemia 24, 1096–1098.

Kosoff, R.E., Aslan, J.E., Kostyak, J.C., Dulaimi, E., Chow, H.Y., Prudnikova, T.Y., Radu, M., Kunapuli, S.P., McCarty, O.J.T., Chernoff, J., 2015. Pak2 restrains endomitosis during megakaryopoiesis and alters cytoskeleton organization. Blood 125, 2995–3005.

Kuter, D.J., 2007. New thrombopoietic growth factors. Blood 109, 4607–4616.

Kuter, D.J., Begley, C.G., 2002. Recombinant human thrombopoietin: basic biology and evaluation of clinical studies. Blood 100, 3457–3469.

Levy, J.H., Neal, M.D., Herman, J.H., 2018. Bacterial contamination of platelets for transfusion: strategies for prevention. Crit. Care 22, 271.

Li, C.Q., Hu, M.Y., Jiang, S.J., Liang, Z.H., Wang, J.M., Liu, Z.H., Wang, H.M.D., Kang, W. Y., 2020. Evaluation procoagulant activity and mechanism of astragalin. Molecules 25, 177.

Li, C.Z., Zheng, L., 2014. The pharmacology and clinical application of thrombopoietin receptor agonists. Int. J. Hematol. 100, 529–539.

Lin, K.H., Li, M.W., Chang, Y.C., Lin, Y.N., Ho, Y.H., Weng, W.C., Huang, C.J., Chang, B. E., Yao, C.L., Lee, H., 2018. Activation of lysophosphatidic acid receptor 3 inhibits megakaryopoiesis in human hematopoietic stem cells and zebrafish. Stem Cells Dev. 27, 216–224.

Lomenick, B., Hao, R., Jonai, N., Chin, R.M., Aghajan, M., Warburton, S., Wang, J.N., Wu, R.P., Gomez, F., Loo, J.A., Wohlschlegel, J.A., Vondriska, T.M., Pelletier, J., Herschman, H.R., Clardy, J., Clarke, C.F., Huang, J., 2009. Target identification using drug affinity responsive target stability (DARTS). Proc. Natl. Acad. Sci. USA 106, 21984–21989.

Maroni, P., 2019. Megakaryocytes in bone metastasis: protection or progression? Cells-Basel 8, 134.

Michel M, R.M., Gonzalez-Lopez, T.J., Alkindi, S.S., Cheze, S., Ghanima, W., Tvedt, T.H. A., Ebbo, M., Terriou, L., Bussel, J.B., Godeau, B., 2020. Use of thrombopoietin receptor agonists for immune thrombocytopenia in pregnancy: results from a multicenter study. Blood 136, 3056-3061.

Molina, D.M., Jafari, R., Ignatushchenko, M., Seki, T., Larsson, E.A., Dan, C., Sreekumar, L., Cao, Y.H., Nordlund, P., 2013. Monitoring drug target engagement in cells and tissues using the cellular thermal shift assay. ScienceScience 341, 84–87.
Nakamura, T., 2008. Elaboration of a novel small molecule, NIP-004, with thrombopoietin mimetic activities. Rinsho Ketsueki 49, 257–262.
Nakamura, T., Miyakawa, Y., Miyamura, A., Yamane, A., Suzuki, H., Ito, M., Ohnishi, Y., Ishiwata, N., Ikeda, Y., Tsuruzoe, N., 2006. A novel nonpeptidyl human c-Mpl activator stimulates human megakaryopoiesis and thrombopoiesis. Blood 107, 4300–4307.
Nicolai, L., Gaertner, F., Massberg, S., 2019. Platelets in host defense: experimental and clinical insights. Trends Immunol. 40, 922–938.
Nogami, W., Yoshida, H., Koizumi, K., Yamada, H., Abe, K., Arimura, A., Yamane, N., Takahashi, K., Yamane, A., Oda, A., Tanaka, Y., Takemoto, H., Ohnishi, Y., Ikeda, Y., Miyakawa, Y., 2008. The effect of a novel, small non-peptidyl molecule butyzamide on human thrombopoietin receptor and megakaryopoiesis. Haematol-Hematol. J. 93, 1495–1504.
Patel-Hett, S., Richardson, J.L., Schulze, H., Drabek, K., Isaac, N.A., Hoffmeister, K., Shivdasani, R.A., Bulinski, J.C., Galjart, N., Hartwig, J.H., Italiano Jr., J.E., 2008. Visualization of microtubule growth in living platelets reveals a dynamic marginal band with multiple microtubules. Blood 111, 4605–4616.
Pleines, I., Dutting, S., Cherpokova, D., Eckly, A., Meyer, I., Morowski, M., Krohne, G., Schulze, H., Gachet, C., Debili, N., Brakebusch, C., Nieswandt, B., 2013. Defective tubulin organization and proplatelet formation in murine megakaryocytes lacking Rac1 and Cdc42. Blood 122, 3178–3187.
Portielje, J.E., Westendorp, R.G., Kluin-Nelemans, H.C., Brand, A., 2001. Morbidity and mortality in adults with idiopathic thrombocytopenic purpura. Blood 97, 2549–2554.
Prihoda, D., Maritz, J.M., Klempir, O., Dzamba, D., Woelk, C.H., Hazuda, D.J., Bitton, D. A., Hannigan, G.D., 2021. The application potential of machine learning and genomics for understanding natural product diversity, chemistry, and therapeutic translatability. Nat. Prod. Rep. 38, 1100–1108.
Sim, X., Poncz, M., Gadue, P., French, D.L., 2016. Understanding platelet generation from megakaryocytes: implications for in vitro-derived platelets. Blood 127, 1227–1233.
Singh, V.K., Kumar, N., Kalsan, M., Saini, A., Chandra, R., 2016. A novel peptide thrombopoietin mimetic designing and optimization using computational approach. Front. Bioeng. Biotech. 4, 69.
Songdej, N., Rao, A.K., 2017. Hematopoietic transcription factor mutations: important players in inherited platelet defects. Blood 129, 2873–2881.
Stasi, R., Bosworth, J., Rhodes, E., Shannon, M.S., Willis, F., Gordon-Smith, E.C., 2010. Thrombopoietic agents. Blood Rev. 24, 179–190.
Su, X.D., Guo, R.H., Yang, S.Y., Kim, Y.H., Kim, Y.R., 2019. Anti-bacterial effects of components from *Sanguisorba officinalis* L. on Vibrio vulnificus and their soluble epoxide hydrolase inhibitory activity. Nat. Prod. Res. 33, 3445–3449.
Svoboda, O., Stachura, D.L., Machonova, O., Pajer, P., Brynda, J., Zon, L.I., Traver, D., Bartunek, P., 2014. Dissection of vertebrate hematopoiesis using zebrafish thrombopoietin. Blood 124, 220–228.
Szalai, G., LaRue, A.C., Watson, D.K., 2006. Molecular mechanisms of megakaryopoiesis. Cell. Mol. Life Sci. 63, 2460–2476.
Teng, J.F., Mei, Q.B., Zhou, X.G., Tang, Y., Xiong, R., Qiu, W.Q., Pan, R., Law, B.Y., Wong, V.K., Yu, C.L., Long, H.A., Xiao, X.L., Zhang, F., Wu, J.M., Qin, D.L., Wu, A.G., 2020. Polyphyllin VI induces caspase-1-mediated pyroptosis via the induction of ROS/NF-kappaB/NLRP3/GSDMD signal axis in non-small cell lung cancer. Cancers 12, 193.
Thon, J.N., Italiano, J.E., 2012. Does size matter in platelet production? Blood 120, 1552–1561.
Wang, L., Zhang, T., Liu, S., Mo, Q., Jiang, N., Chen, Q., Yang, J., Han, Y.W., Chen, J.P., Huang, F.H., Li, H., Zhou, J., Luo, J.S., Wu, J.M., 2022. Discovery of a novel megakaryopoiesis enhancer, ingenol, promoting thrombopoiesis through PI3K-Akt signaling independent of thrombopoietin. Pharmacol. Res. 177,106096.
Woods, B., Chen, W., Chiu, S., Marinaccio, C., Fu, C.L., Gu, L., Bulic, M., Yang, Q., Zouak, A., Jia, S.X., Suraneni, P.K., Xu, K.L., Levine, R.L., Crispino, J.D., Wen, Q.J., 2019. Activation of JAK/STAT signaling in megakaryocytes sustains myeloproliferation in vivo. Clinic. Cancer Res. 25, 5901–5912.
Xie, C., Zhao, H., Bao, X., Fu, H., Lou, L., 2018a. Pharmacological characterization of hetrombopag, a novel orally active human thrombopoietin receptor agonist. J. Cell. Mol. Med. 22, 5367–5377.
Xie, C.Y., Zhao, H.J., Bao, X.B., Fu, H.Y., Lou, L.G., 2018b. Pharmacological characterization of hetrombopag, a novel orally active human thrombopoietin receptor agonist. J. Cell. Mol. Med. 22, 5367–5377.
Xu, M., Luo, L., Du, M.Y., Tang, L., Hu, Y., Mei, H., 2020. Fibrinogen levels are associated with bleeding in patients with primary immune thrombocytopenia. Platelets 31, 763–770.
Yan, X.H., Guo, Y.W., 2004. Two new ellagic acid glycosides from leaves of Diplopanax stachyanthus. J. Asian Nat. Prod. Res. 6, 271–276.
Yao, Y.Z., Wang, Z.H., Li, L., Lu, K., Liu, R.Y., Liu, Z.Y., Yan, J., 2019. An ontology-based artificial intelligence model for medicine side-effect prediction: taking traditional chinese medicine as an example. Comput. Math. Method. 2019, 8617503.
Zhu, L.J., Chen, L., Bai, C.F., Wu, A.G., Liang, S.C., Huang, F.H., Cao, S.S., Yang, L., Zou, W.J., Wu, J.M., 2020. A rapid and sensitive UHPLC-MS/MS method for the determination of ziyuglycoside I and its application in a preliminary pharmacokinetic study in healthy and leukopenic rats. Biomed. Pharmacother. 123, 109756.